Supporting Information

A Stereoelectronic Effect on Turn Formation Due to Proline Substitution in Elastin-Mimetic Polypeptides.

Wookhyun Kim, R. Andrew McMillan, James P. Snyder and Vincent P. Conticello[*]

[*]To whom correspondence should e addressed. E-mail: vcontic@emory.edu. Telephone: (404) 727-2779. Fax: (404) 727-6586

[†]Department of Chemistry, Emory University, 1515 Dickey Drive, Atlanta, GA 30322

[‡]Bioengineering Branch, NASA Ames Research Center, Moffett Field, CA 94035

Figure S1. Expansion of the two-dimensional ^{1}H-^{1}H NOESY NMR spectra depicting the Val(αH)-Pro(δH) cross-peaks associated with the *trans* configuration of the Val-Pro peptidyl bond for **elastin-1** (**A**), **elastin-2** (**B**), and **elastin-3** (**C**). Note the absence of a strong Val(αH)-Pro(αH) cross-peak corresponding to a *cis* Val-Pro peptidyl bond configuration.

A.

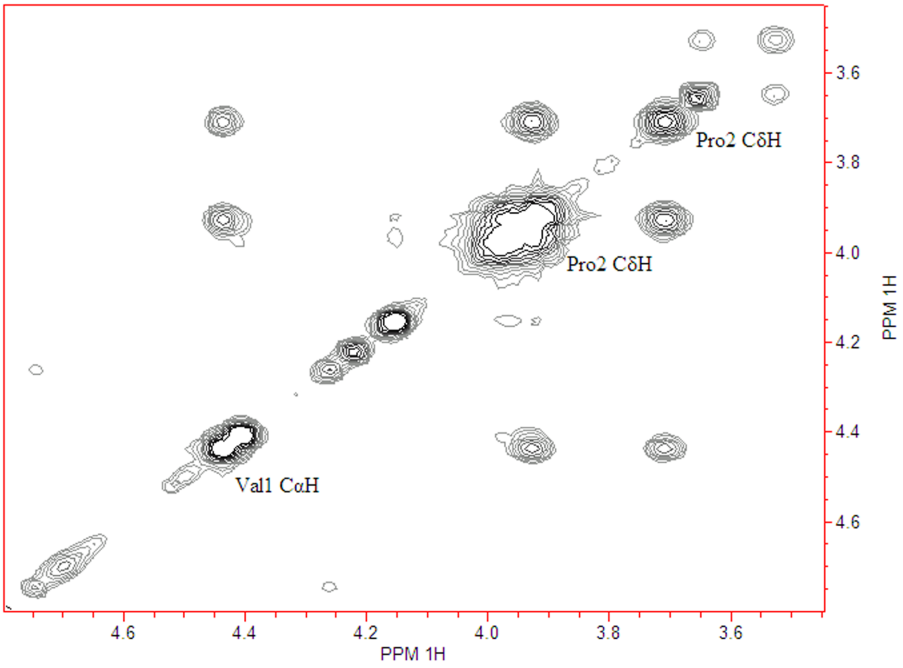

B.

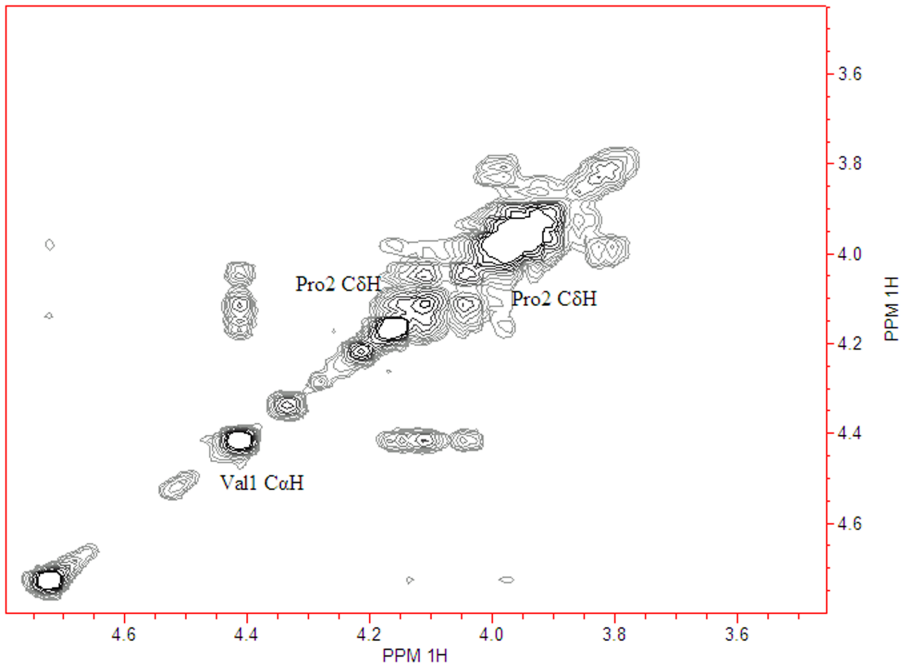
Pro2 CδH
Pro2 CδH
Val1 CαH
3.6
3.8
4.0
4.2
4.4
4.6
PPM 1H
4.6
4.4
4.2
4.0
3.8
3.6
PPM 1H

C.

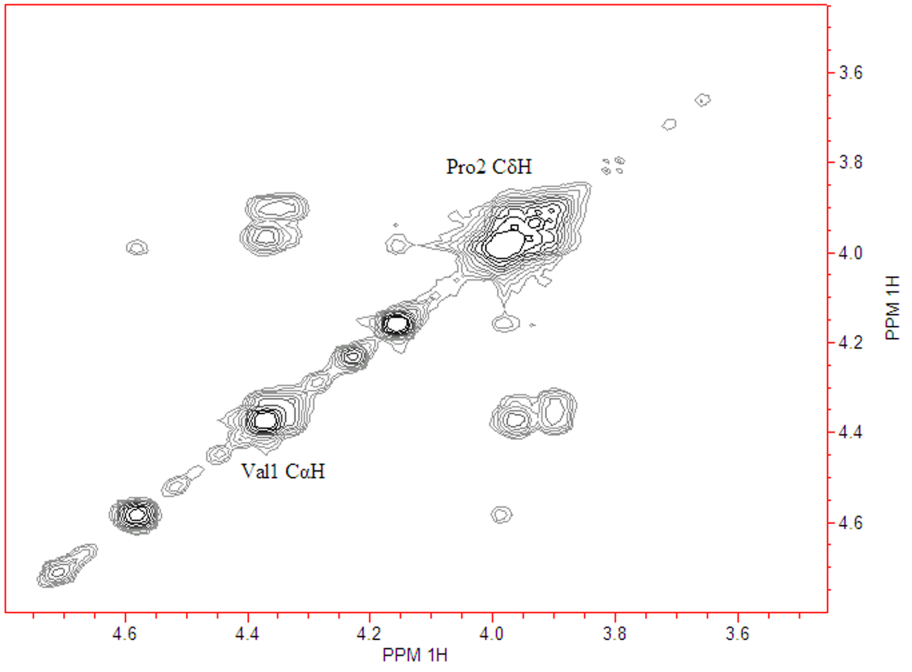
Pro2 CδH
Val1 CαH
3.6
3.8
4.0
4.2
4.4
4.6
PPM 1H
4.6
4.4
4.2
4.0
3.8
3.6
PPM 1H

Figure S2. Expansion of the two-dimensional ^{1}H-^{1}H NOESY NMR spectra depicting the HN-Hα cross-peaks that were employed to confirm the spectroscopic assignments of the non-proline residues in the pentapeptide repeats of the elastomeric domains of **elastin-1** (**A**), **elastin-2** (**B**), and **elastin-3** (**C**).

A.

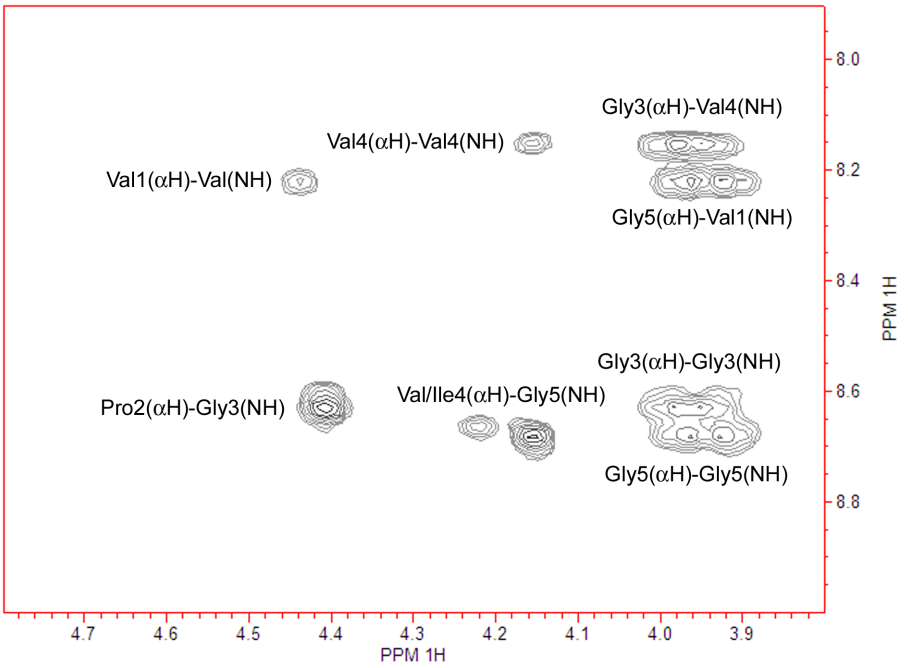

B.

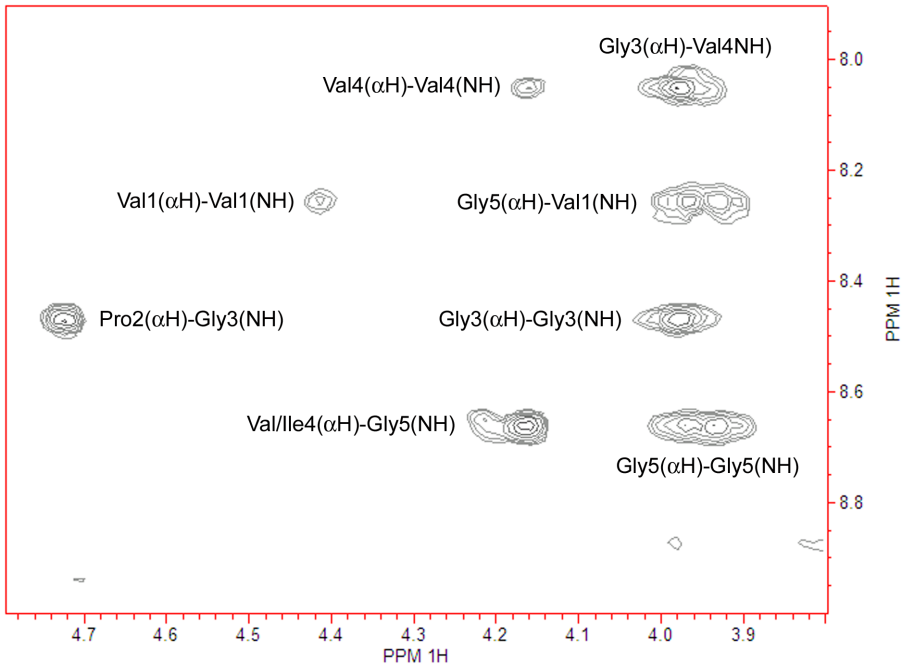
Gly3(αH)-Val4NH)
Val4(αH)-Val4(NH)
Val1(αH)-Val1(NH)
Gly5(αH)-Val1(NH)
Pro2(αH)-Gly3(NH)
Gly3(αH)-Gly3(NH)
Val/Ile4(αH)-Gly5(NH)
Gly5(αH)-Gly5(NH)
8.0
8.2
8.4
8.6
8.8
PPM 1H
4.7
4.6
4.5
4.4
4.3
4.2
4.1
4.0
3.9
PPM 1H

C.

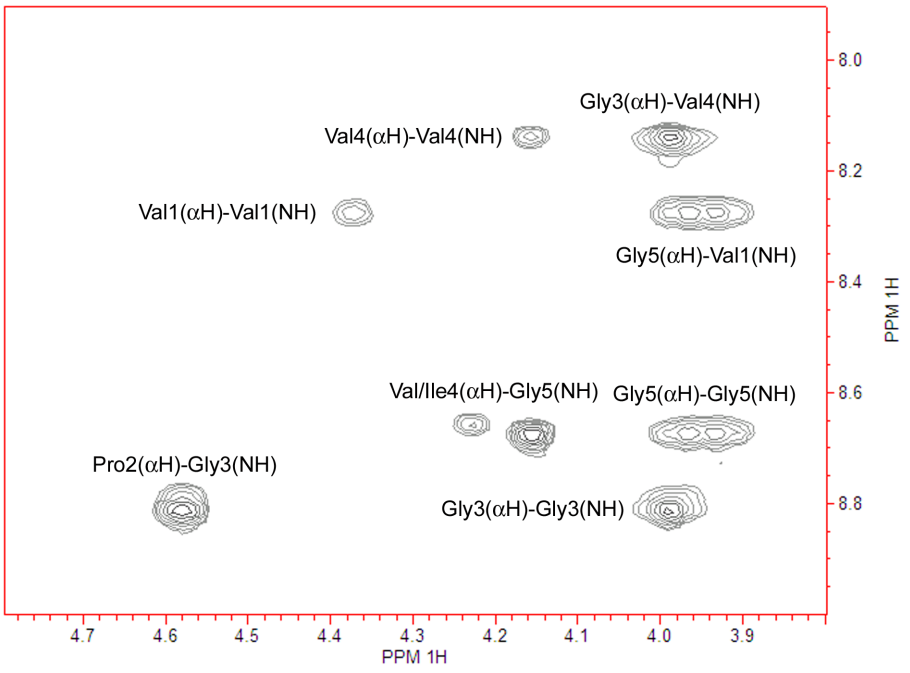
Gly3(αH)-Val4(NH)
Val4(αH)-Val4(NH)
Val1(αH)-Val1(NH)
Gly5(αH)-Val1(NH)
Val/Ile4(αH)-Gly5(NH)
Gly5(αH)-Gly5(NH)
Pro2(αH)-Gly3(NH)
Gly3(αH)-Gly3(NH)
8.0
8.2
8.4
8.6
8.8
PPM 1H
4.7
4.6
4.5
4.4
4.3
4.2
4.1
4.0
3.9
PPM 1H

Figure S3. Calculated structures of conformer pairs for inverse γ-turn structures derived from the model peptide segment (MeCO-Pro-Gly-NHMe) incorporating (*2S*,*4S*)-4-fluoroproline (top) and (*2S*,*4R*)-4-fluoroproline (bottom). The labels indicate the ring pucker associated with C^{γ} position of the pyrrolidine ring and the position of the fluorine substituent. Geometries were derived from structural optimization at the Beck3LYP/6311+G(2d,p) level of theory.

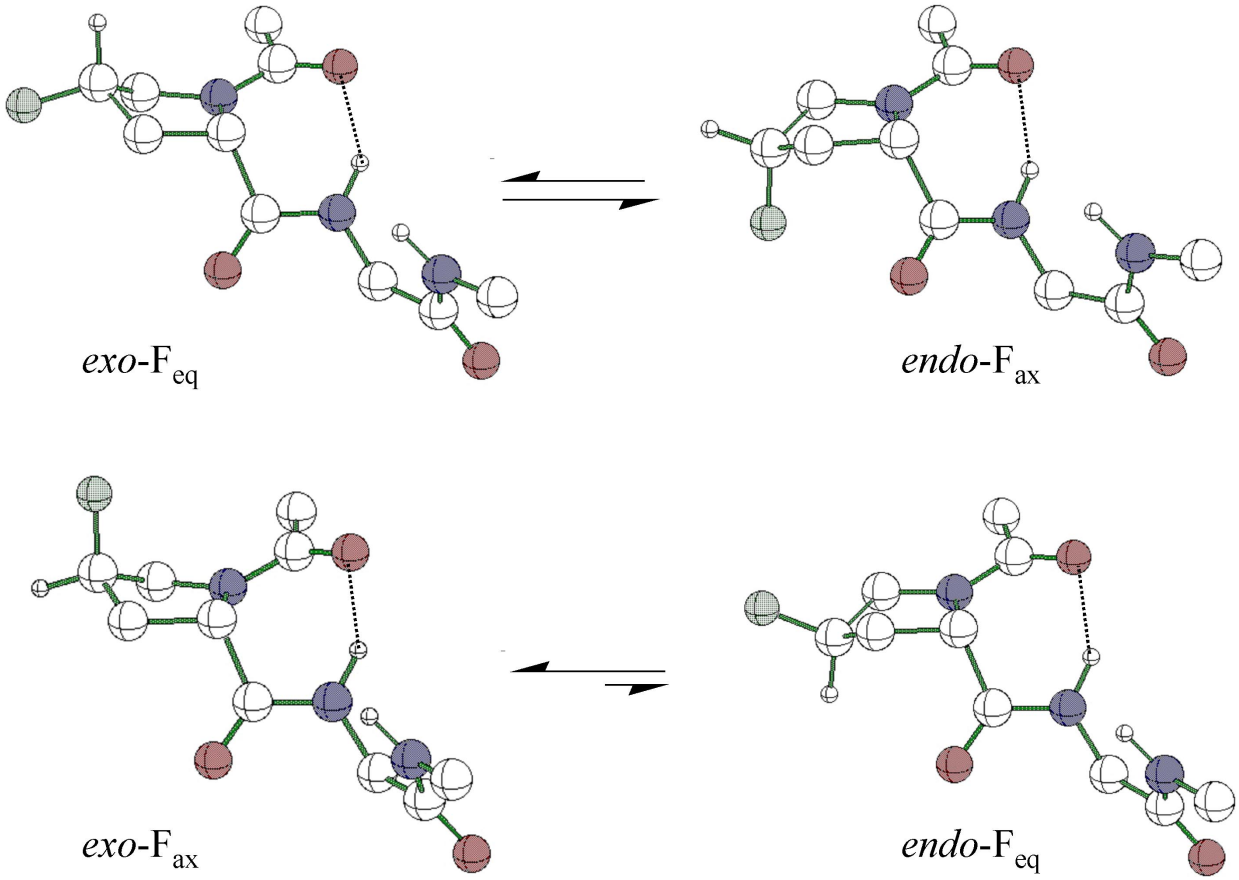

Table S1. Type-I β-turns in the VPGVG truncated peptide; energy differences (ΔE, kcal/mol), ϕ,ψ angles (deg) and ^{15}N chemical shifts (ppm).

Beck3LYP/6-31G* opt[a]								
	Total E, au	ΔE_1	6-311+G(2d,p)[b]	ΔE_2	Pro ϕ and ψ[c]		Gly ϕ and ψ[c]		δ (N-H)[d,e]
exo	-781.279 423	0.6	-781.529 489	0.4	-66.0	-21.8	-103.2	16.9	96.2
endo	-781.280 313	0.0	-781.530 159	0.0	-79.8	-1.8	-105.5	13.2	104.2
exo-F_{eq}	-880.507 427	2.0	-880.797 713	1.7	-66.6	-21.7	-103.9	17.4	96.5
endo-F_{ax}	-880.510 664	0.0	-880.800 406	0.0	-75.9	-6.8	-107.6	14.9	102.6
exo-F_{ax}	-880.509 888	0.0	-880.800 559	0.0	-67.8	-20.7	-103.2	16.8	97.1
endo-F_{eq}	-880.508 173	1.1	-880.798 268	1.4	-80.4	0.2	-106.0	12.5	103.6
Beck3LYP/6-311+G* opt[f]									
	Total E, au	ΔE_3	6-311+G(2d,p)[g]	ΔE_4	Pro ϕ and ψ[c]		Gly ϕ and ψ[c]		δ (N-H)[d]
exo	-781.489 586	0.4	-781.530 155	0.4	-66.8	-18.8	-97.5	10.2	95.1[h] 105.9[i]
endo	-781.490 207	0.0	-781.530 807	0.0	-78.3	-3.7	-99.8	7.8	102.1[h] 113.8[i]
exo-F_{eq}	-880.757 107	1.8	-880.798 527	1.8	-68.1	-18.1	-97.3	10.3	95.4[h] 106.0[i]
endo-F_{ax}	-880.759 936	0.0	-880.801 461	0.0	-74.1	-8.9	-103.1	10.4	100.5[h] 111.5[i]
exo-F_{ax}	-880.759 852	0.0	-880.801 367	0.0	-70.5	-15.1	-97.5	9.5	96.4[h] 107.5[i]
endo-F_{eq}	-880.757 524	1.5	-880.799 024	1.6	-78.5	-2.8	-100.3	7.8	95.1[h] 105.9[i]

[a] Beck3LYP/6-31G*//Beck3LYP/6-31G*

[b] Beck3LYP/6311+G(2d,p)//Beck3LYP/6-31G*

[c] ϕ angle (O)C-N-C-C(O); ψ angle N-C-C(O)-N

[d] Calculated ^{15}N chemical shifts for N-H bonds of the Gly residue of (MeCO-Xaa-Gly-NHMe) in ppm relative to liquid NH_3 at 25 °C (absolute shielding 244.6 ppm is set to zero ppm); see Experimental Methods for details.

[e] MPW1PW91/6-311G*//Beck3LYP/6-31G*

[f] Beck3LYP/6-311+G*//Beck3LYP/6-311+G*

[g] Beck3LYP/6-311+G(2d,p)//Beck3LYP/6-311+G*

[h] MPW1PW91/6-311G*//Beck3LYP/6-311+G*

[i] PBE/6-311+G(2d,p)//Beck3LYP/6-311+G*

Table S2. Type-II β-turns in the VPGVG truncated peptide; energy differences (ΔE, kcal/mol), ϕ,ψ angles (deg) and ^{15}N chemical shifts (ppm).

Beck3LYP/6-31G* opt[a]							
	Total E, au	ΔE_1	6-311+G(2d,p)[b]	ΔE_2	Pro ϕ and ψ[c]	Gly ϕ and ψ[c]	δ (N-H)[d,e]
exo	-781.282 827	0.3	-781.532 882	0.0	-60.5 123.4	104.6 -16.1	111.7
endo	-781.283 337	0.0	-781.532 497	0.2	-70.7 113.5	108.6 -12.0	116.1
exo-F_{eq}	-880.511 004	0.0	-880.801 349	0.0	-60.2 124.8	104.6 -16.5	115.0
endo-F_{ax}	-880.508 684	1.5	-880.798 090	2.1	-62.1 133.7	100.6 -18.3	111.0
exo-F_{ax}	-880.514 147	0.0	-880.805 096	0.0	-61.9 121.2	105.7 -15.6	116.1
endo-F_{eq}	-880.512 803	0.9	-880.802 235	1.8	-71.2 112.1	109.7 -11.3	116.7
Beck3LYP/6-311+G* opt[f]							
	Total E, au	ΔE_3	6-311+G(2d,p)[g]	ΔE_4	Pro ϕ and ψ[c]	Gly ϕ and ψ[c]	δ (N-H)[d]
exo	-781.492 951	0.0	-781.533 453	0.0	-57.7 127.5	99.8 -14.2	111.7[h] 122.7[i]
endo	-781.492 830	0.08	-781.533 325	0.08	-65.1 126.3	97.2 -10.0	110.8[h] 121.8[i]
exo-F_{eq}	-880.760 646	0.0	-880.801 957	0.0	-58.8 127.1	100.1 -13.7	112.2[h] 123.2[i]
endo-F_{ax}	-880.757 554	0.8	-880.799 121	1.8	-61.0 133.1	97.7 -15.2	109.1[h] 120.6[i]
exo-F_{ax}	-880.764 367	0.0	-880.805 750	0.0	-60.1 124.9	100.6 -12.9	113.1[h] 123.9[i]
endo-F_{eq}	-880.761 920	1.5	-880.803 256	1.6	-65.5 125.3	99.9 -10.9	112.1[h] 123.1[i]

[a] Beck3LYP/6-31G*//Beck3LYP/6-31G*

[b] Beck3LYP/6311+G(2d,p)//Beck3LYP/6-31G*

[c] ϕ angle (O)C-N-C-C(O); ψ angle N-C-C(O)-N

[d] Calculated ^{15}N chemical shifts for N-H bonds of the Gly residue of (MeCO-Xaa-Gly-NHMe) in ppm relative to liquid NH_3 at 25 °C (absolute shielding 244.6 ppm is set to zero ppm); see Experimental Methods for details.

[e] MPW1PW91/6-311G*//Beck3LYP/6-31G*

[f] Beck3LYP/6-311+G*//Beck3LYP/6-311+G*

[g] Beck3LYP/6-311+G(2d,p)//Beck3LYP/6-311+G*

[h] MPW1PW91/6-311G*//Beck3LYP/6-311+G*

[i] PBE/6-311+G(2d,p)//Beck3LYP/6-311+G*

Table S3. Gamma turns in the VPGVG truncated peptide; energy differences (ΔE, kcal/mol), ϕ,ψ angles (deg) and ^{15}N chemical shifts (ppm).

Beck3LYP/6-31G* opt[a]							
	Total E, au	ΔE_1	6-311+G(2d,p)[b]	ΔE_2	Pro ϕ and ψ[c]	Gly ϕ and ψ[c]	δ (N-H)[d,e]
exo	-781.280 667	1.2	-781.530 318	1.0	-82.0 76.6	-122.1 14.4	113.6
endo	-781.282 518	0.0	-781.531 852	0.0	-83.7 72.7	-121.5 14.8	112.7
exo-F_{eq}	-880.509 150	0.3	-880.799 060	0.0	-82.1 76.1	-121.9 14.5	113.5
endo-F_{ax}	-880.509 689	0.0	-880.798 999	0.04	-82.4 58.6	-117.1 14.6	107.6
exo-F_{ax}	-880.512 361	0.0	-880.803 026	0.0	-83.6 75.7	-123.3 14.8	113.6
endo-F_{eq}	-880.511 499	0.5	-880.801 107	1.2	-83.7 75.2	-121.4 14.2	111.1
Beck3LYP/6-311+G* opt[f]							
	Total E, au	ΔE_3	6-311+G(2d,p)[g]	ΔE_4	Pro ϕ and ψ[c]	Gly ϕ and ψ[c]	δ (N-H)[d]
exo	-781.489 832	1.0	-781.530 860	1.0	-82.0 76.6	-122.1 14.4	111.8[h] 125.5[i]
endo	-781.491 480	0.0	-781.532 457	0.0	-83.7 72.7	-121.5 14.8	110.5[h] 124.0[i]
exo-F_{eq}	-880.757 870	0.0	-880.799 711	0.1	-82.4 76.8	-115.5 9.8	113.5[h] 125.0[i]
endo-F_{ax}	-880.757 723	0.1	-880.799 937	0.0	-81.6 54.3	-107.6 8.7	107.7[h] 121.3[i]
exo-F_{ax}	-880.761 878	0.0	-880.803 764	0.0	-83.5 76.6	-116.0 9.3	111.6[h] 125.0[i]
endo-F_{eq}	-880.760 043	1.2	-880.801 745	1.3	-84.0 76.1	-113.4 7.8	111.2[h] 124.4[i]

[a] Beck3LYP/6-31G*//Beck3LYP/6-31G*

[b] Beck3LYP/6311+G(2d,p)//Beck3LYP/6-31G*

[c] ϕ angle (O)C-N-C-C(O); ψ angle N-C-C(O)-N

[d] Calculated ^{15}N chemical shifts for N-H bonds of the Gly residue of (MeCO-Xaa-Gly-NHMe) in ppm relative to liquid NH_3 at 25 °C (absolute shielding 244.6 ppm is set to zero ppm); see Experimental Methods for details.

[e] MPW1PW91/6-311G*//Beck3LYP/6-31G*

[f] Beck3LYP/6-311+G*//Beck3LYP/6-311+G*

[g] Beck3LYP/6-311+G(2d,p)//Beck3LYP/6-311+G*

[h] MPW1PW91/6-311G*//Beck3LYP/6-311+G*

[i] PBE/6-311+G(2d,p)//Beck3LYP/6-311+G*

Complete Citation for Reference 59:

59. Gaussian 03, Revision C.02, Frisch, M. J.; Trucks, G. W.; Schlegel, H. B.; Scuseria, G. E.; Robb, M. A.; Cheeseman, J. R.; Montgomery, Jr., J. A.; Vreven, T.; Kudin, K. N.; Burant, J. C.; Millam, J. M.; Iyengar, S. S.; Tomasi, J.; Barone, V.; Mennucci, B.; Cossi, M.; Scalmani, G.; Rega, N.; Petersson, G. A.; Nakatsuji, H.; Hada, M.; Ehara, M.; Toyota, K.; Fukuda, R.; Hasegawa, J.; Ishida, M.; Nakajima, T.; Honda, Y.; Kitao, O.; Nakai, H.; Klene, M.; Li, X.; Knox, J. E.; Hratchian, H. P.; Cross, J. B.; Bakken, V.; Adamo, C.; Jaramillo, J.; Gomperts, R.; Stratmann, R. E.; Yazyev, O.; Austin, A. J.; Cammi, R.; Pomelli, C.; Ochterski, J. W.; Ayala, P. Y.; Morokuma, K.; Voth, G. A.; Salvador, P.; Dannenberg, J. J.; Zakrzewski, V. G.; Dapprich, S.; Daniels, A. D.; Strain, M. C.; Farkas, O.; Malick, D. K.; Rabuck, A. D.; Raghavachari, K.; Foresman, J. B.; Ortiz, J. V.; Cui, Q.; Baboul, A. G.; Clifford, S.; Cioslowski, J.; Stefanov, B. B.; Liu, G.; Liashenko, A.; Piskorz, P.; Komaromi, I.; Martin, R. L.; Fox, D. J.; Keith, T.; Al-Laham, M. A.; Peng, C. Y.; Nanayakkara, A.; Challacombe, M.; Gill, P. M. W.; Johnson, B.; Chen, W.; Wong, M. W.; Gonzalez, C.; and Pople, J. A.; Gaussian, Inc., Wallingford CT, 2004.